The Sensitivity of Simulated Convective Storms to Variations in Prescribed Single-Moment Microphysics Parameters that Describe Particle Distributions, Sizes, and Numbers

CHARLES COHEN AND EUGENE W. MCCAUL JR.

Universities Space Research Association, Huntsville, Alabama

(Manuscript received 15 April 2005, in final form 7 December 2005)

ABSTRACT

The sensitivity of cloud-scale simulations of deep convection to variations in prescribed microphysics parameters is studied, using the single-moment scheme in the Regional Atmospheric Modeling System (RAMS) model. Realistic changes were made to the shape parameters in the gamma distributions of the diameters of precipitating hydrometeors and of cloud droplets, in the number concentration of cloud droplets, and in the mean size of the hail and graupel. Simulations were performed with two initial soundings that are identical except for their temperature. The precipitation rate at the ground is not very sensitive to changes in the value of the shape parameter used for all precipitating hydrometeors (rain, hail, graupel, snow, and aggregates) or to the mean size of the hail and graupel, owing to counteracting effects. For example, with a larger shape parameter value, there is a greater production of precipitation by collection of cloud water, but also a larger rate of evaporation of the liquid precipitation. However, with a larger shape parameter value, the greater production of precipitation by collection and the increased evaporation result in more low-level cooling by the downdraft. Specifying larger hail and graupel results in less low-level cooling by the downdraft. The simulation with the cold initial sounding showed a change in storm propagation velocity when the specified sizes of hail and graupel were increased, but this did not occur when the warm initial sounding was used. With a larger shape parameter for cloud water or with a larger number concentration of cloud droplets, there is less autoconversion and less collection of cloud water and, consequently, much less precipitation at the ground and denser cirrus anvils. While the number concentration of cloud droplets can be forecast in some models with parameterized microphysics, at present the shape parameter for cloud water cannot and must, therefore, be carefully selected.

1. Introduction

Any parameterization of microphysical processes requires that some physical quantities be specified. Even in two-moment schemes, in which the mean size of the hydrometeors can be computed from the forecast mixing ratio and the forecast number concentration, some assumption must be made about the shape of the distribution of the hydrometeor sizes in each category. Single-moment schemes, such as the one used in this study, must additionally make some assumption that enables the model to determine the mean diameter of each species. For simulations of observed storms, it may be possible to derive values for these specified quantities from observations, but in operational forecasting or in theoretical studies, no such guidance is available. This naturally leads to the question of how suitable the models are for these purposes. In studies of the use of cloud-scale models for operational forecasting, Brooks et al. (1992) and Elmore et al. (2002a,b, 2003) generated ensembles of simulations with slightly different initial conditions, finding considerable sensitivity to those varying conditions. However, the models are also sensitive to variations in arbitrarily specified microphysics parameters (McCumber et al. 1991; van den Heever and Cotton 2004; Gilmore et al. 2004a). Cloud-scale models are useful in theoretical studies only if the conclusions of those studies are not very sensitive to reasonable variations in the specified quantities.

Our purpose here is to examine how sensitive cloud-scale simulations of deep convection are to reasonable variations in adjustable microphysics parameters, using a recent set of Regional Atmospheric Modeling System

Corresponding author address: Charles Cohen, Universities Space Research Association, 320 Sparkman Dr., Huntsville, AL 35805.
E-mail: cohen@usra.edu

© 2006 American Meteorological Society

(RAMS) simulations (McCaul et al. 2005) as an example. In the RAMS model (Pielke et al. 1992; Walko et al. 1995), hydrometeors in each category are described by a gamma distribution:

$$n(D) = \frac{N_t}{\Gamma(\nu)} \left(\frac{D}{D_n}\right)^{\nu-1} \frac{1}{D_n} \exp\left(-\frac{D}{D_n}\right), \quad (1)$$

where the number density n is a function of the diameter D. Here, N_t is the total number concentration, Γ is the gamma function, ν is the shape parameter of the gamma distribution, and D_n is the characteristic diameter. Using the equation

$$\overline{m} = \frac{\rho_a r}{N_t}, \quad (2)$$

where $\overline{m}$ is mean mass of the hydrometeor species, ρ_a is the air density, and r is the hydrometeor mixing ratio, it becomes apparent that only two of the three parameters, ν, N_t, and D_n, must be fixed when N_t is not forecast. (Note that N_t is forecast only for pristine crystals in the present simulations.) In RAMS, ν is always given a constant value. Here, N_t is specified for cloud water, and the standard practice for other hydrometeors has been to specify, instead of D_n, the diameter of the particle with mean mass, $D_{\overline{m}}$. This can be related to D_n by using Eq. (5) of Walko et al. (1995) to express the mean mass of the hydrometeor category as

$$\overline{m} = \alpha_m D_n^{\beta_m} \frac{\Gamma(\nu + \beta_m)}{\Gamma(\nu)} = \alpha_m D_{\overline{m}}^{\beta_m}, \quad (3)$$

where the mass of a particle with diameter D is $\alpha_m D^{\beta_m}$, as in Eq. (6) of Walko et al. (1995). For rain, hail, and graupel, the constants α_m and β_m are derived by assuming that the hydrometeors are spherical with densities of 1000, 900, and 300 kg m^{-3}, respectively.

McCaul et al. (2005) used $\nu = 1.5$, and for $D_{\overline{m}}$ they used the default values in RAMS of 0.1 cm for rain and graupel and 0.3 cm for hail. Hail is conventionally defined as having a diameter of at least 0.5 cm (Glickman 2000). However, as Meyers et al. (1997) explain, the mean diameter of hail in RAMS is smaller than would be expected because the hail category in the model also includes frozen drops, which are smaller than hail. Truncating the hail size distribution at 0.5 cm, as suggested by Curic and Janc (1997), would therefore not be appropriate in RAMS.

The values that are selected for these adjustable parameters should ideally depend on the types of clouds being simulated. For example, McCumber et al. (1991) explain that frozen rain, not large hail, is actually typical in the Tropics. Therefore, for simulations of maritime tropical convection, they advise increasing the intercept N_0 in an exponential distribution for hail to better reflect a rain distribution. This would be difficult to do, however, in a model with a large domain that may include many types of storms.

Calculations of ν and $D_{\overline{m}}$ from observed raindrop size distributions have produced conflicting results. Tokay and Short (1996), for example, fitted gamma distribution functions to maritime tropical raindrop spectra, and found that ν and $D_{\overline{m}}$ (using our notation) both increase with increasing surface rainfall rate, ranging from $D_{\overline{m}} = 0.076$ cm and $\nu = 2.7$ for very light rain to $D_{\overline{m}} = 0.16$ cm and $\nu = 9.9$ for extremely heavy rain. The RAMS default value of $D_{\overline{m}} = 0.10$ cm for rain applies, in their data, to moderate rain, with $\nu = 3.9$. Nzeukou et al. (2004) derived very similar results. However, Zhang et al. (2003) and Brandes et al. (2003), using a notation similar to that of Tokay and Short (1996), examine a relationship between the distribution slope Λ (mm^{-1}), and the shape parameter μ, where

$$\Lambda = 0.0365\mu^2 + 0.735\mu + 1.935. \quad (4)$$

Translating between (4) and (1), $\Lambda = D_n^{-1}$ and $\mu = \nu - 1$. Equations (3) and (4) together produce values of $D_{\overline{m}}$ for rain restricted to the range of 0.09 cm to slightly over 0.11 cm when ν varies from 1 to 11. We can conclude from these observational studies that $D_{\overline{m}} = 0.1$ cm is a typical value for rain.

Observational studies have shown a wide range of values for ν in distributions of raindrops. For example, in addition to the results of Tokay and Short (1996), quoted above, Ulbrich (1983) reviewed previous studies that showed ν ranging from 1.4 to 2.63 for thunderstorms and from -2.42 to 6.04 for showers. For convective rain, Bringi et al. (2003) showed values of ν between 2 and 9.9, while Martinez and Gori (1999) derived negative values of ν.

McCumber et al. (1991) compared different microphysics models that included at most three ice categories, such as cloud ice, snow, and hail. Their advice that the number of ice categories should be increased has since been adopted for the RAMS model. Number concentrations of each hydrometeor type should also be predicted, they suggest, especially for simulations of squall lines that include convective and stratiform regions. In the present simulations of deep convection, we use a model that predicts number concentration only of pristine ice crystals, but this does not seriously conflict with the advice of McCumber et al. (1991), because none of the simulations include extensive stratiform anvils.

It is difficult to select values for the adjustable parameters from observations, because D in (1) ranges

from zero to infinity and applies to only one hydrometeor species. An observed size distribution may include particles from more than one of the categories of hydrometeors in RAMS. Mitchell et al. (1996), for example, use an exponential distribution for ice crystals smaller than 150 μm, and a gamma distribution for particles larger than 150 μm. Their bimodal size spectra may be equivalent to the sum of two gamma distributions in RAMS: one of pristine crystals with $\nu = 1$ and one of snow with $\nu > 1$. Our version of RAMS can accommodate this.

Additional problems with the use of observed size distributions in developing modeling procedures are that the observed distributions generally do not neatly fit a mathematical function and that they are not constant over time and space, as required for a microphysics parameterization like the one in RAMS. Martinez and Gori (1999) and Uijlenhoet et al. (2003) each obtained different values of ν for rain for two different ways of fitting a gamma distribution to data. Figure 12 of Bringi et al. (2002) shows a large variation with time of the shape parameter of a gamma distribution for rain during the passage of a squall line. Variation of microphysical parameters over space within a storm is shown by Brandes et al. (2004a,b). Fraile et al. (2003) and Giaiotti et al. (2001) show that an exponential distribution of hailstones aloft will change to a gamma distribution at the ground as a result of melting.

The issue raised by McCumber et al. (1991), referred to above, of the number of ice categories in a microphysics parameterization can be interpreted in two different ways. This is exemplified by the work of Gilmore et al. (2004a), who examine the effect of changing the sizes of hail and graupel. In their model, hydrometeor diameters are exponentially distributed [using $\nu = 1$ in Eq. (1)]. They specify different values of the constant N_0 (which equals $N_t D_n^{-1}$ for an exponential distribution). For one hydrometeor category, which they label "hail/graupel," they specify one of only two different values of the particle density, 400 or 900 kg m^{-3}. They interpret this category as including both graupel and hail, and thus demonstrate (as did McCumber et al. 1991) that there is too wide an observed range of N_0 and particle density to reasonably represent both hail and graupel in a single category (M. Gilmore 2005, personal communication). In contrast, we believe, with Straka and Mansell (2005), Tao et al. (2003), and Lang et al. (2004), that by specifying the density as either 400 or 900 kg m^{-3}, and specifying some parameter related to the size distribution, a hail–graupel category includes either hail or graupel, but not both. With our interpretation, the selections by Gilmore et al. (2004a) of N_0 and particle density without regard to the properties of the initial sounding lead to some possibly unlikely combinations of dynamics and microphysics within a storm. As explained by Lang et al. (2004), strong updrafts are more likely to generate hail, while weak updrafts produce graupel.

With a different version of the RAMS model than we are using here, van den Heever and Cotton (2004) demonstrate significant impacts on the storm dynamics and microphysics of changing the specified mean diameter of hail. In the present study, we investigate the sensitivity of the simulations to variations in specified values of N_t, $D_{\overline{m}}$, and ν. Sensitivity to changes in the latter parameter has not previously been examined.

Until it becomes feasible to replace models with parameterized microphysics with bin models (Khain et al. 2000; Lynn et al. 2005a,b), selecting values for adjustable parameters in microphysics parameterizations will always be necessary and will never be easy.

2. Methods

In this study, we use version 3b of the RAMS model (RAMS 3b), configured as in McCaul and Cohen (2002), but with a number of modifications and improvements, which are listed in McCaul et al. (2005). In addition to solving for the three Cartesian velocities, ice-liquid water potential temperature (Tripoli and Cotton 1981), and pressure, the model also forecasts mixing ratios of rain, hail, graupel, pristine ice, snow, and aggregates, and employs a diagnostic equation to obtain temperature and the mixing ratios of water vapor and cloud water. Particle number concentration is forecast for pristine ice.

We use RAMS with a square domain, 75 km on a side, with a horizontal grid interval of 500 m, and a vertically stretched grid with spacing ranging from 250 m at the ground to 750 m at 20 km in altitude. The two soundings (Fig. 1) used in the horizontally uniform initial state are designed to have identical pseudoadiabatic buoyancy profiles for lifted parcels, and the same profiles of wind and relative humidity, but different mean temperatures. Therefore, the warmer sounding has more precipitable water. Each sounding has a pseudoadiabatic CAPE of 2000 J kg^{-1}, a PBL depth of 1.6 km, buoyancy and shear concentrated in the lower troposphere, and a semicircular hodograph with a radius of 12 m s^{-1}. Simulations using these same soundings are examined in section 3a of McCaul et al. (2005). Convection is initiated with a spheroidal warm bubble, as in McCaul et al. (2005).

In the first two experiments, we change ν in (1) simultaneously for all precipitating hydrometeor species (rain, hail, graupel, snow, and aggregates) from the 1.5 used in our previous work to 5, and we then increase

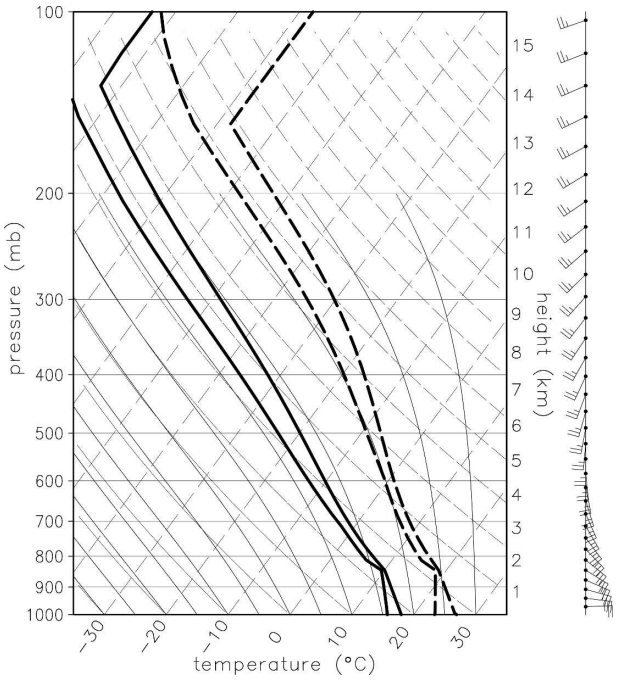

FIG. 1. Initial cold (solid) and warm (dashed) soundings. The altitudes along the right edge are valid only for the cold sounding, with similar altitudes occurring at somewhat larger pressures for the warm sounding. The wind barbs, which are a function of height, are shown for the cold sounding.

$D_{\overline{m}}$ by 150% for both graupel and hail to 0.25 and 0.75 cm, respectively, and leave $D_{\overline{m}}$ unchanged for other species.

Observations of shallow clouds (Miles et al. 2000; Costa et al. 2000) have shown the value of ν for cloud water ν_c to vary widely. We therefore also test the sensitivity of the simulations to changes in this parameter, increasing it to 5 from our customary value of 1.

The default value of the cloud droplet number concentration N_{tc} in RAMS is 300 cm^{-3}, which is typical of maritime conditions. Because the effect of increasing N_{tc} is qualitatively the same for different amounts of increase, we show results for N_{tc} = 2000 cm^{-3}, a number appropriate for clouds forming in polluted air (Eagan et al. 1974a,b; Andreae et al. 2004).

Cloud microphysics parameterization

RAMS computes the rate of collection of hydrometeors with a lookup table, as described in Walko et al. (1995, section 2.5). The tables are correct only when ν = 1.5 for precipitating species, so here we use the collection tables that we recomputed, as reported in McCaul et al. (2005), for all values of ν, so that they more closely conform to the stochastic collection equation [Walko et al. (1995), Eq. (46)]. Examining the efficiencies of collection of cloud water by rain also necessitated a change in the model formulation.

In RAMS 3b the efficiency of collection of cloud water by any precipitating hydrometeor is given by the ratio of D_n of cloud droplets to 14 μm, but not more than 1. In the present simulations, D_n is very rarely larger than 14 μm for cloud droplets. With this formula, therefore, the collection efficiency varies with changes to the microphysics parameters.

The methods of computing autoconversion and of computing accretion of cloud water by rain have changed from RAMS 3b to version 4.4 (RAMS 4.4). In the newer version, these two processes are combined into a lookup table derived from output from a bin model, as described by Feingold et al. (1998). This newer method was used by McCaul and Cohen (2002) and McCaul et al. (2005). Examining model results that use the newer lookup tables for accretion reveals that they imply a collection efficiency that does not vary with the size of the cloud droplets, in contrast to the collection efficiencies shown in Fig. 3 of Beard and Ochs (1984). For the present simulations, we have therefore restored the old method (described above) of computing accretion of cloud water by rain, which we believe is more realistic. However, this would not change any of our previous results, because simulations using our default values of ν_c = 1 and N_{tc} = 300 cm^{-3} and ν = 1.5 for rain are nearly identical for the two methods of computing accretion of cloud water by rain. As shown in section 3c, the effects on the autoconversion rate of changing either ν_c or N_{tc} are at least qualitatively in line with expectations.

There is no consensus on how to compute collection efficiencies for accretion of cloud water by rain (Khain et al. 2000, section 2.2). As Beard et al. (2002) noted, "For most cloud drop sizes, the collection efficiency has not been measured." With ν_c = 1, if N_{tc} is increased from 300 to 2000 cm^{-3}, D_n and the mean diameter of the cloud droplets both decrease by 47%, for a fixed ρ_a and r, leading to a smaller collection efficiency using the method of RAMS 3b. However, if ν_c is increased from 1 to 5 with a fixed N_{tc}, D_n decreases by 69%, but the mean diameter increases by 55%. As shown in Fig. 2, with the larger ν_c the modal diameter of the number density increases, but because the distribution is narrower, more of the mass is in small cloud droplets. In RAMS 3b, therefore, increasing ν_c leads to a decreased efficiency of rain collecting cloud droplets. In RAMS 4.4, the collection efficiency for any category of frozen precipitation collecting cloud droplets is an increasing function of the mean mass of the cloud droplets and, thus, does not depend on ν_c when $D_{\overline{m}}$ is a constant [Eq. (3)].

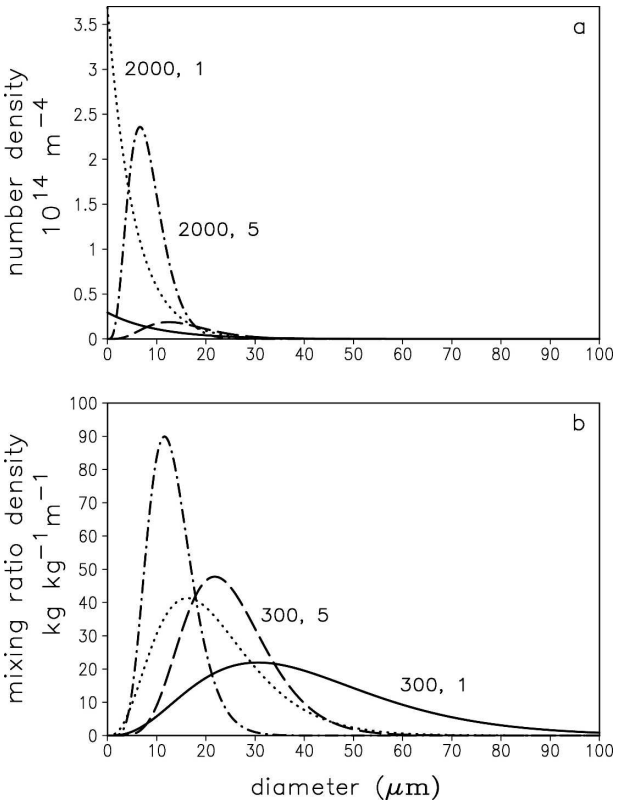

FIG. 2. (a) Size distribution of cloud droplets for N_{tc} = 300 cm^{-3}, for ν = 1 (solid) and ν = 5 (dashed), and for N_{tc} = 2000 cm^{-3}, for ν = 1 (dotted) and ν = 5 (dot–dashed). (b) Mixing ratio density for the distributions of cloud droplets shown in (a). These were computed by multiplying each point in the size distributions by the mass of the cloud droplet. Labels in the curves show N_{tc}, ν.

3. Results

The simulations are, to varying extents, sensitive to changes in the microphysics formulation, but not sensitive enough to influence the primary conclusions of McCaul et al. (2005), whose purpose was to examine how simulations of deep convection differ if the temperature of the initial state is changed. For example (Fig. 3), the maximum vertical velocities in the simulated updrafts are consistently larger in the upper troposphere with the cold soundings, while the strongest downdrafts near the ground are invariably stronger with the warm soundings. Our more general purpose here, as discussed in section 1, is to determine if realistic variations in microphysics parameters have other effects on the simulations, apart from the particular aims of McCaul et al. (2005).

Multiplying $D_{\overline{m}}$ by 2.5 for hail and graupel makes more of a difference in the simulations than does increasing ν from 1.5 to 5 for rain, hail, graupel, snow, and aggregates. We begin by demonstrating why the rates of precipitation at the ground are not very sensitive to the value of ν for precipitating species, but then we show why modelers nevertheless need to carefully select the value of ν. Next, we draw similar conclusions from a comparison of simulations with different values of $D_{\overline{m}}$ for hail and graupel. Finally, we examine the effect of varying N_{tc} and of ν_c.

a. Sensitivity to ν for precipitation

For each hydrometeor species in the present simulations, $D_{\overline{m}}$ is specified. Figure 4a shows four gamma distributions of hailstones, all with a mass density of 1 g m^{-3}, for ν equal to 1.5 and 5, and for $D_{\overline{m}}$ equal to 0.30 cm (the default value) and 0.75 cm. Increasing ν produces a narrower and less positively skewed distribution with a larger mode, fewer small particles, and fewer large particles. For $D_{\overline{m}}$ = 0.30 cm, the mean diameter of the hail increases from 0.19 to 0.25 cm when ν increases from 1.5 to 5, while the modal diameter increases from 0.06 to 0.20 cm. When $D_{\overline{m}}$ increases by 150%, the mean and modal diameters also increase by 150%, for either value of ν.

Next, we compute the rate of collection of cloud water by a hailstone of each diameter, using N_{tc} = 300 cm^{-3} (the default value in RAMS), and a cloud droplet diameter of 20 μm. When this is multiplied by the size distributions, we obtain collection densities (Fig. 4b), showing the rate of collection of cloud droplets as a function of the diameter of the hailstone. The areas under these curves are the total collection rates. Hailstones smaller than 0.1 cm collect very little cloud water, even when, with ν = 1.5, they are present in large numbers. Increasing ν from 1.5 to 5 causes only a 14% increase in the collection rate, because with ν = 1.5 the small numbers of hailstones larger than 0.6 cm have large rates of collection.

From (2) and (3), we see that for a given air density and a given hydrometeor mixing ratio, the hydrometeor number concentration does not vary with ν when $D_{\overline{m}}$ is specified as a constant. However, it can be demonstrated, using Eq. (5) of Walko et al. (1995), that the mean surface area of the hydrometeors is 26% larger when ν is increased from 1.5 to 5 while $D_{\overline{m}}$ is held constant. These two results, combined with the different distributions of fall speeds for the two values of ν, determine how the rate of evaporation of rain changes with ν. With a larger fall speed, the greater wind speed relative to the hydrometeor increases the evaporation rate, but the hydrometeors spend less time evaporating before they reach the ground.

In fact, averaged over space and time during the second hour of the simulations, the most prominent effect of increasing ν from 1.5 to 5 for precipitating hydro-

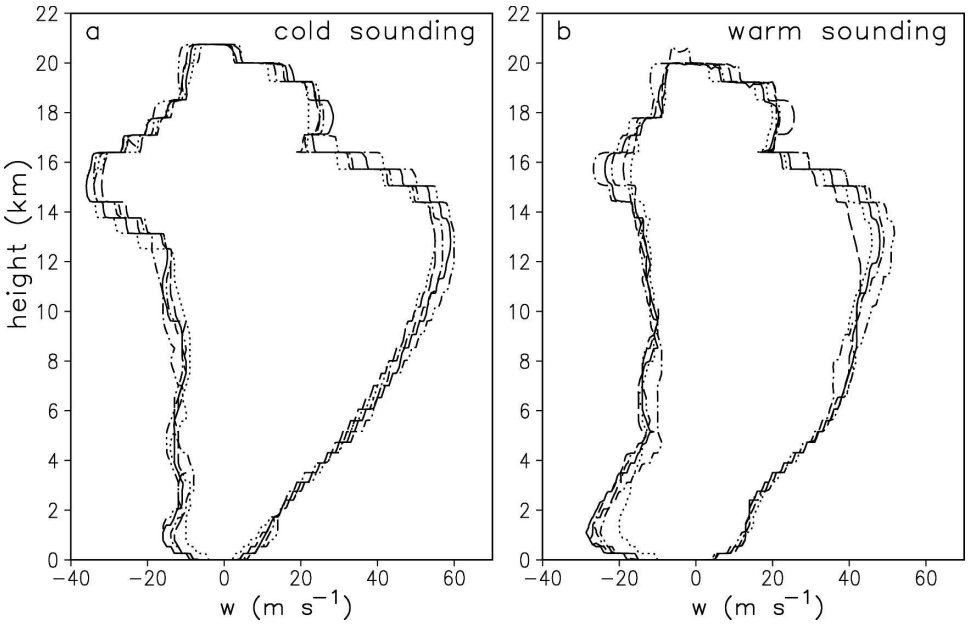

FIG. 3. Minimum and maximum vertical velocities in clouds during the second hour of the control simulations (solid), $N_{tc} = 2000$ cm^{-3} (dashed), $\nu = 5$ for cloud water (dotted), larger hail and graupel (dot–dashed), and $\nu = 5$ for precipitation (dot–dot–dashed); with the (a) cold and (b) warm soundings. The vertical velocities are rounded to the nearest integer.

meteors is a greater evaporation of rain (Fig. 5), leading to slightly less precipitation at the ground (Fig. 6). The negative curves in Fig. 5 display evaporation below 2.2 km and sublimation above 2.2 km for simulations with the cold soundings; the boundary is at 4.1 km for the simulations with the warm soundings. For the simulations with the cold soundings, increasing ν from 1.5 to 5 results in a 14% increase in the vertically averaged production of precipitation and an 81% increase in the vertically averaged evaporation of rain. With the warm sounding, the changes are smaller, with increases of 5% in the production of precipitation and 38% in the evaporation. The differences in the precipitation rates at the ground are not large because, as we have seen, there is a larger collection rate with the larger ν. If we compare the sum of the collection of cloud water by all precipitating species plus the autoconversion to the homogeneous freezing of cloud water, we see that with a larger ν for precipitating hydrometeors, the conversion of cloud water to precipitation is more efficient (Fig. 7). This is because of the greater rate of collection of cloud water by rain (not shown). If the collection of cloud water were shown in Fig. 7 without the autoconversion, the figure would look similar, because the autoconversion is much smaller in magnitude than the collection and changes less with the change in ν.

Convective heating [e.g., Eq. (21) of Frank and Cohen (1985)] is difficult to compute directly in a limited-area model, but we can examine some components. Despite the small difference in the precipitation at the ground, the larger rate of evaporation with the larger ν causes a substantial increase in the cooling near the surface. This can be inferred from Fig. 8, which shows the vertical flux in convective downdrafts of perturbation virtual potential temperature, defined as $M_d\theta'_v$, where M_d is the downdraft mass flux and θ'_v is the perturbation of $\theta_v = \theta(1 + 1.608q_v)/(1 + q_v)$ from the initial state. Convective heating by compensating subsidence (not shown) is not significantly affected by the increase in ν.

b. Sensitivity to the size of hail and graupel

For a given mixing ratio of hail or graupel, the number concentration, which is not forecast in the present model, decreases when $D_{\overline{m}}$ increases, causing a decrease in the collection rate. Specifically, when $D_{\overline{m}}$ increases by 150% for hail and graupel, without changing ν, the mass-weighted mean terminal velocity increases by 58%, the mean cross-sectional area of the hydrometeor is multiplied by 6.25, and the hydrometeor number concentration is multiplied by 0.064. The net result is a decrease in the collection rate (the areas under the curves in Fig. 4b) by 37%, for either value of ν. This should be expected; for a single hailstone of diameter D, the collection rate is very close to being proportional

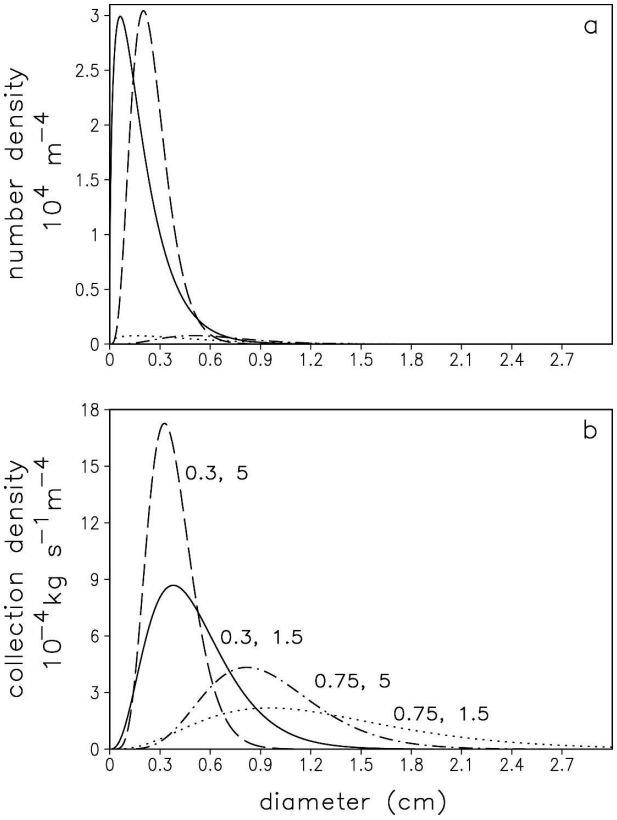

FIG. 4. (a) Gamma distributions of hailstones with mass density 1 g m^{-3}, and (b) the collection density for the distributions of hail shown in (a) collecting a monodisperse distribution of cloud droplets with number concentration 300 cm^{-3} and diameter 20 μm. The curves are for hail distributions with $D_{\overline{m}}$ = 0.30 cm, ν = 1.5 (solid); $D_{\overline{m}}$ = 0.30 cm, ν = 5 (dashed); $D_{\overline{m}}$ = 0.75 cm, ν = 1.5 (dotted); $D_{\overline{m}}$ = 0.75 cm, ν = 5 (dot–dashed). Labels on the curves show $D_{\overline{m}}$, ν.

to $D^{2.5}$ (the terminal velocity, which is proportional to the square root of the diameter, multiplied by the cross-sectional area), while the mass is proportional to D^3. Larger hailstones, therefore, have lower collection rates per unit mass. In the simulations, the actual changes in the collection rates resulting from an increase in $D_{\overline{m}}$ depend on the mixing ratios of the collector and collected species.

The smaller collection rate per unit mass for larger hailstones is largely compensated by the fact that, when less cloud water is collected by hail, there is more of it available to be collected by graupel, whose peak concentration is at a slightly higher altitude (Fig. 9). Still, there is less precipitating condensate and more non-precipitating condensate in the updrafts, averaged over time and space, with the larger $D_{\overline{m}}$ (Fig. 10). This indicates a slower conversion of cloud water to precipitation, but it is partly due to the fact that with the larger $D_{\overline{m}}$, because the fall speeds of hail and graupel are 58% larger, they spend less time aloft. Gilmore et al. (2004a, their Fig. 8) similarly noted less hail and more snow and cloud ice with the larger average particle size that results from a smaller specified N_0 in their exponential distributions.

With fewer and larger hailstones with the larger $D_{\overline{m}}$, there is less total surface area, causing slower melting, as explained by van den Heever and Cotton (2004), and consequently more hail and less rain, and therefore less evaporation, at low levels. However, because of the slower conversion of cloud water to precipitation, there is, despite the increase in fall speeds, only a small difference in the precipitation at the ground when the average size of the hail and graupel is increased (Fig. 6). The wider range of precipitation rates in the simulations of Gilmore et al. (2004a) is probably a consequence of their larger range of specified particle sizes and densities. Despite the small sensitivity of the precipitation rates in our simulations to an increase in $D_{\overline{m}}$ of hail and graupel, the smaller rate of evaporation with the larger $D_{\overline{m}}$ causes a significant decrease in the cooling by downdrafts, as can be inferred from Fig. 8. Gilmore et al. (2004a) and van den Heever and Cotton (2004) obtained similar results.

Storm motion is one of the most easily observed characteristics of storms and is of great importance operationally. Furthermore, storm motions can potentially serve as a useful tool for validation of cloud model results. However, methods of forecasting storm motion are often based on a combination of observations and theory (Bunkers et al. 2000), and are still prone to error. Is it possible that microphysical considerations might play a role in influencing storm motions, thereby explaining some of the error in current storm motion forecasting methods?

The simulations of van den Heever and Cotton (2004) show little impact on storm motions. However, our own simulations show some influence of the specified size of the hydrometeors on the speed and direction of storm propagation. This occurs primarily with the cold soundings. Figures 11a–f show horizontal fields near the ground at 45 min for the $D_{\overline{m}}$ = 0.3 cm and $D_{\overline{m}}$ = 0.75 cm experiments, just as the propagation velocities of the storms in the two simulations are beginning to differ. In the control run, the precipitation aloft, with its smaller terminal velocities, is advected farther ahead of the gust front (Figs. 11a and 11b) and evaporates in the undisturbed warm air. Although this does not change the equivalent potential temperature (Figs. 11c and 11d), it does cool the air ahead of the gust front (Figs. 11e and 11f) and add condensate loading, resulting in a weaker buoyancy gradient and less convergence at the gust front. Ten minutes later (not shown), it is

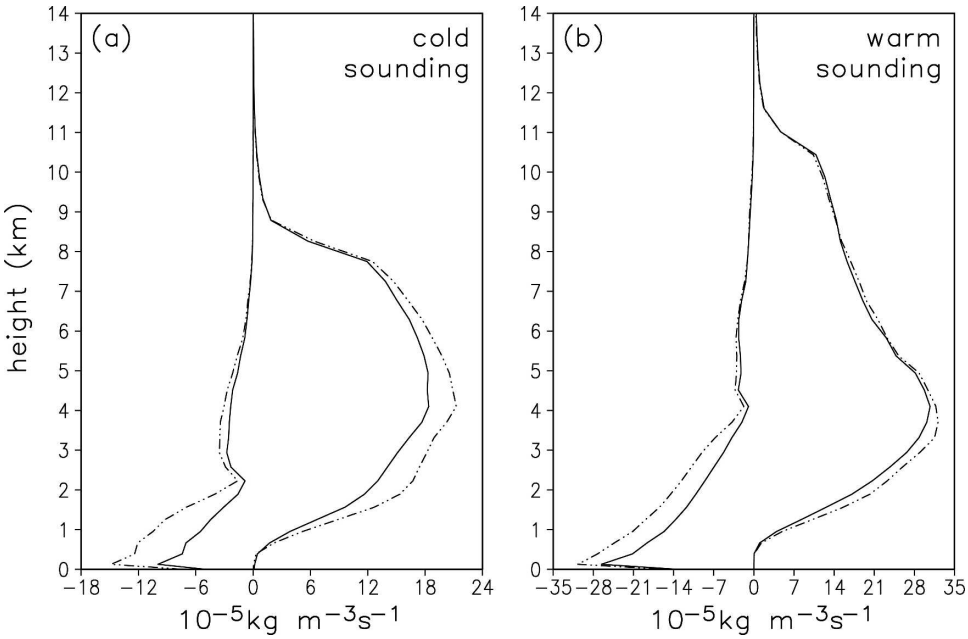

FIG. 5. Production of precipitation (positive numbers) and evaporation of rain plus sublimation of frozen precipitation (negative numbers) for the control simulations (solid) and with $\nu = 5$ for precipitating species (dot–dot–dashed), horizontally averaged over the whole domain for the second hour, for the (a) cold and (b) warm soundings. Production of precipitation is the sum of autoconversion, collection of cloud water and pristine crystals, aggregation of pristine crystals, condensation and deposition onto precipitation, and the conversion of pristine crystals to snow described by Eq. (69) of Walko et al. (1995).

only with the larger hail and graupel that an additional updraft has formed at the gust front between the left and right movers. This soon merges with the right mover, effectively forming a storm with a downdraft beneath the updraft (Fig. 11h), in contrast to the control storm (Fig. 11g), where the downdraft, which is northwest of the updraft, is driving the updraft toward the southeast relative to the moving domain. Relative

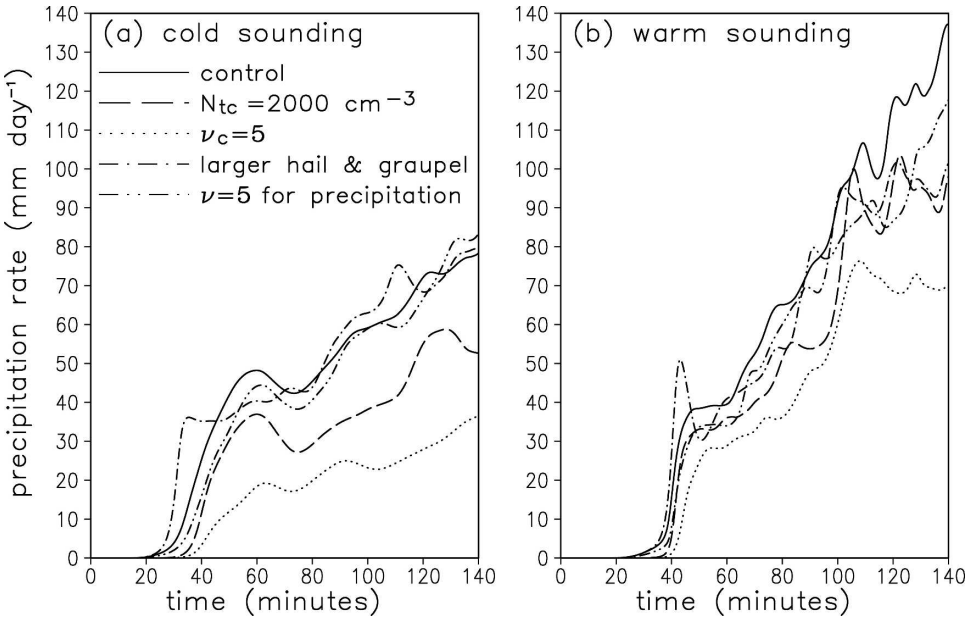

FIG. 6. Time series of precipitation rate at the ground, horizontally averaged over the whole domain, for the control simulations (solid), $N_{tc} = 2000$ cm^{-3} (dashed), $\nu_c = 5$ (dotted), larger hail and graupel (dot–dashed), and $\nu = 5$ for precipitation (dot–dot–dashed); with the (a) cold and (b) warm soundings.

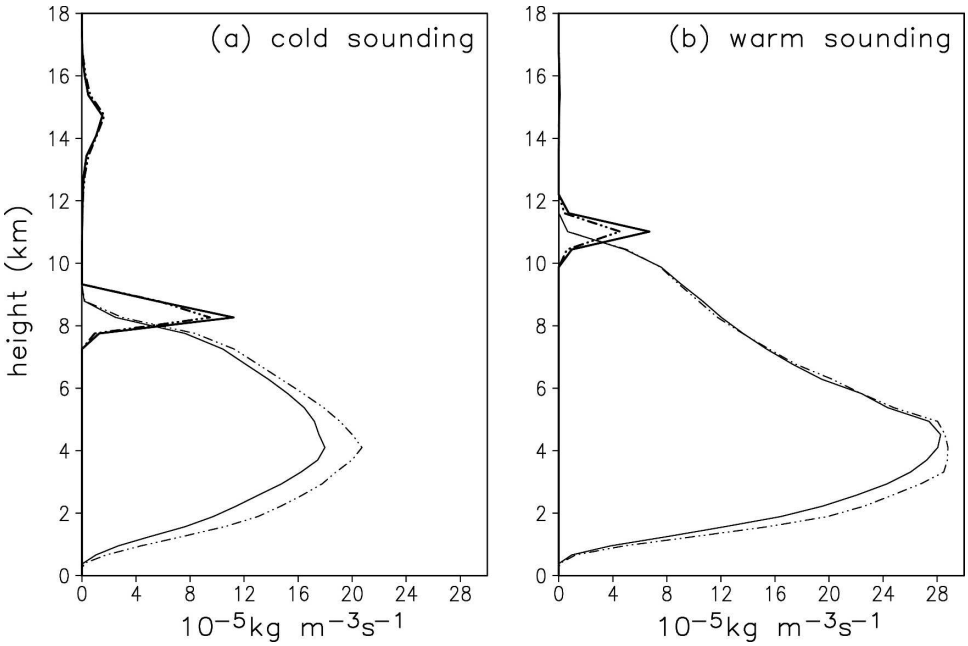

FIG. 7. Collection of cloud water by all precipitating species plus autoconversion (thin) and homogeneous freezing of cloud water (thick) for the control simulations with $\nu = 1.5$ (solid) and with $\nu = 5$ (dot–dot–dashed) for precipitating species, horizontally averaged over the whole domain for the second hour, for the (a) cold and (b) warm soundings.

to the ground, the right movers propagate at 4.2 m s^{-1} toward 344° for the control simulation, and 6.5 m s^{-1} toward 341° with the larger hail and graupel. However, this difference in propagation speed may not be significant, because it is about the same magnitude as the temporal standard deviations of storm motion found by Kirkpatrick and McCaul (2004) in their simulations using a CAPE of 2000 J kg^{-1}, similar to the present study.

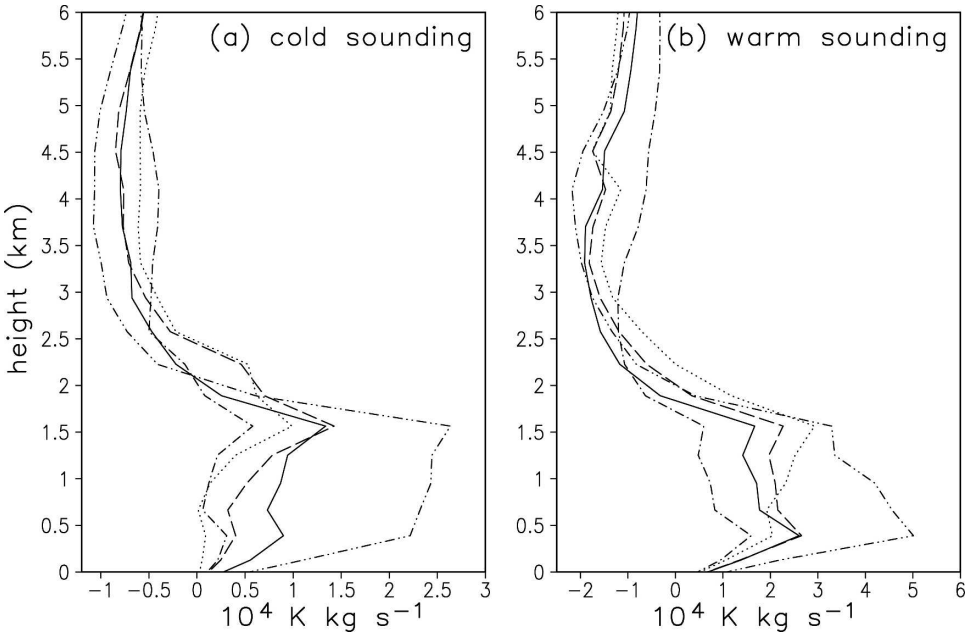

FIG. 8. Perturbation virtual potential temperature flux (10^4 K kg s^{-1}) in convective downdrafts, horizontally averaged over the whole domain during the second hour, for the control simulations (solid), N_{tc} =2000 cm^{-3} (dashed), $\nu_c = 5$ (dotted), larger hail and graupel (dot–dashed), and $\nu = 5$ for precipitation (dot–dot–dashed); with the (a) cold and (b) warm soundings.

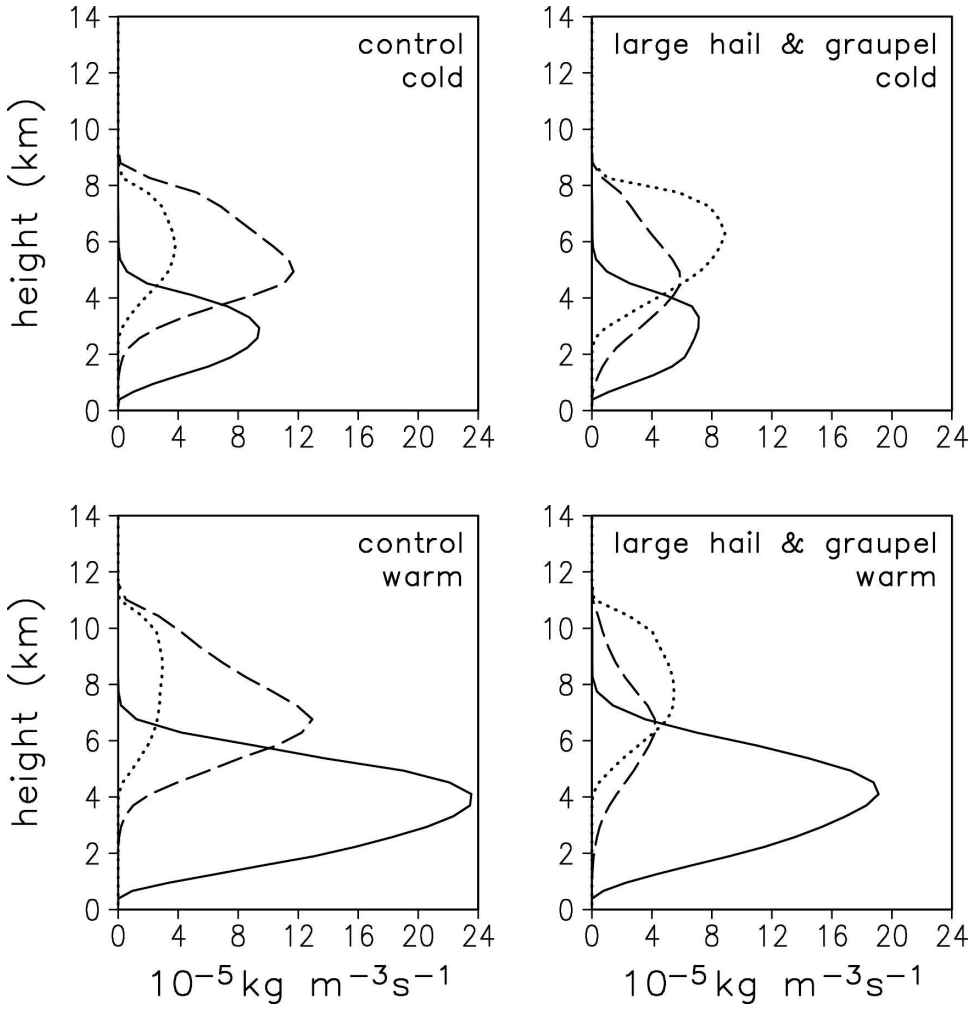

FIG. 9. Collection of cloud water by rain (solid), hail (dashed), and graupel (dotted), horizontally averaged over the second hour, for (left) the control simulations and (right) with the larger hail and graupel, for the (top) cold and (bottom) warm soundings.

With the larger hail and graupel, the downdrafts are weaker, and the gust front does not drive the left mover as rapidly to the northwest. Relative to the ground, the left movers propagate at 14.5 m s^{-1} for the control simulation and 13.2 m s^{-1} with the larger hail and graupel, both toward 320°. As a result, the left and right movers diverge less rapidly with the larger hail and graupel (Figs. 11g and 11h).

The motions of the right and left movers display sensitivity to the size of the hail and graupel only for the simulations with the cold sounding. With the warm sounding, low-level downdrafts are stronger (McCaul et al. 2005). However, as with the cold sounding, the downward flux of cold air is weaker with the larger hail and graupel, because of the decreased evaporation discussed above. In the control simulation with the warm sounding (Fig. 12a), convergence into the tops of strong downdrafts at 45 min advects the condensate toward the updraft, largely negating the effect of the smaller terminal velocity illustrated in Figs. 11a and 11b. With the larger hail and graupel (Fig. 12b), the downdrafts are weaker and shallower, and this condensate can spread farther east. This influence of hail size on downdrafts is relatively ineffective in the simulations with the cold sounding, where the downdrafts are weaker.

c. *Sensitivity to N_{tc} and ν_c*

Because the effects of increasing either N_{tc} or ν_c are qualitatively similar, these experiments are examined together. As we will see, the increase in the shape parameter has a significant effect, despite the fact that it has been studied less often. We begin with the simulations with the cold initial sounding, which are quite sensitive to changes in N_{tc} or ν_c, and then explain why

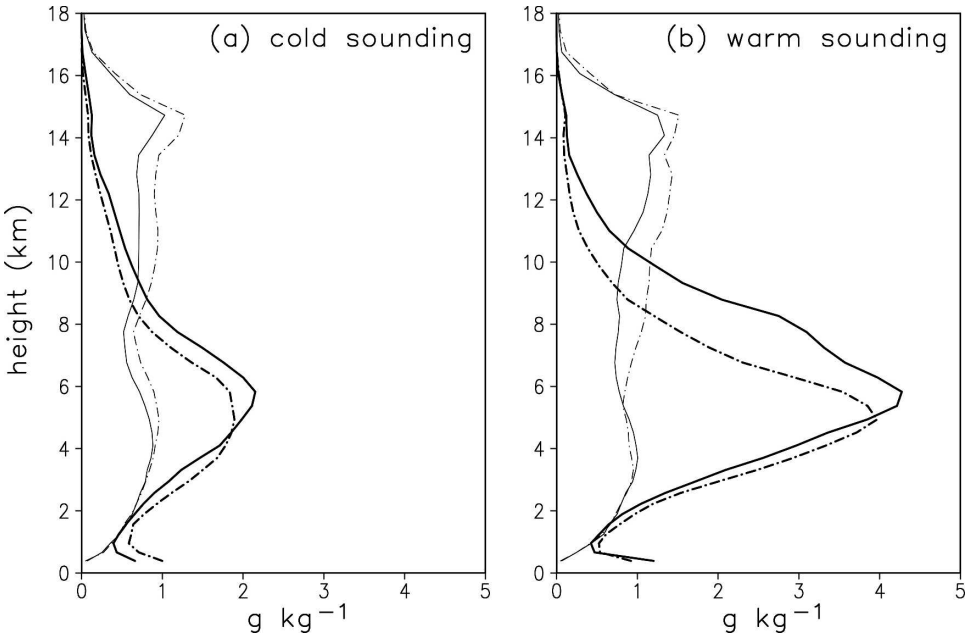

FIG. 10. Rain + hail + graupel (thick) and cloud water + snow + aggregates + pristine crystals (thin) in updrafts for the control simulations (solid) and with the larger hail and graupel (dot–dashed), horizontally averaged over the whole domain for the second hour, for the (a) cold and (b) warm soundings.

the warmer clouds are less sensitive to these changes. It should be remembered that there is an important distinction between varying N_{tc} and varying ν_c. While the former can be forecast in some models with parameterized microphysics (Saleeby and Cotton 2004), at present the latter cannot.

For a given size distribution of the collector species and a given mixing ratio of cloud water, the rate of collection of cloud water [Eq. (46) of Walko et al. (1995)] is a function of the collection efficiency, which is smaller for smaller cloud droplets. With the present model, this reduced efficiency occurs with an increase in N_{tc} or in ν_c, as discussed in section 2a. As the value of ν_c becomes very large, the distribution approaches a monodisperse one, and the autoconversion rate decreases (Liu and Daum 2004). We should also expect less autoconversion with the smaller drops that accompany a larger N_{tc} (Gerber 1996). With less rain generated by autoconversion, collection of cloud water by precipitation will, of course, proceed more slowly.

With the larger N_{tc} or ν_c, there is indeed less autoconversion and less collection of cloud water, and the peak in the vertical profile of the collection of cloud water is shifted to a higher altitude (Fig. 13). Consequently, more of the cloud water reaches the -40°C level in the updraft, where it freezes to become pristine ice crystals. Figure 14 shows the horizontally averaged updraft heating rates due to the release of latent heat of fusion (K s^{-1}) averaged over the second hour of each simulation, divided by the mean upward velocity in clouds. After multiplying by 1000, this is the heating per kilometer of rise of an updraft parcel. Rain freezes near -10°C, riming of cloud water occurs from 0° up to -40°C, and whatever cloud water is still liquid freezes homogeneously at -40°C. The maxima at -40°C in the curves in Fig. 14 are due to the sum of homogeneous freezing and deposition onto the resulting pristine ice crystals. This is the source of the cirrus anvil, while the freezing at lower levels produces frozen precipitation.

With the larger value of either N_{tc} or ν_c, the most significant impacts are the decrease in freezing plus deposition at -10°C and the increase at -40°C. In conjunction with this, there is much less precipitation at the ground (Fig. 6a) and denser cirrus anvils. Our results therefore verify the conjectures of Andreae et al. (2004) and Crutzen (2004) that, with a larger N_{tc}, the latent heating is larger in proportion to the rate of rainfall at the ground, and much of the latent heating occurs higher in the clouds. The slower conversion of cloud water to precipitation with a larger N_{tc} is consistent with observations (Rosenfeld 1999, 2000).

Khain et al. (1999), in their bin model simulations, show that with a high aerosol concentration, which results in a larger N_{tc}, warm rain is less intense, but rain that derives from melting of graupel or of frozen drops is more intense. In our simulations of deep convection there is a smaller rainfall rate with a larger N_{tc} because of the reduced collection rates and upward displace-

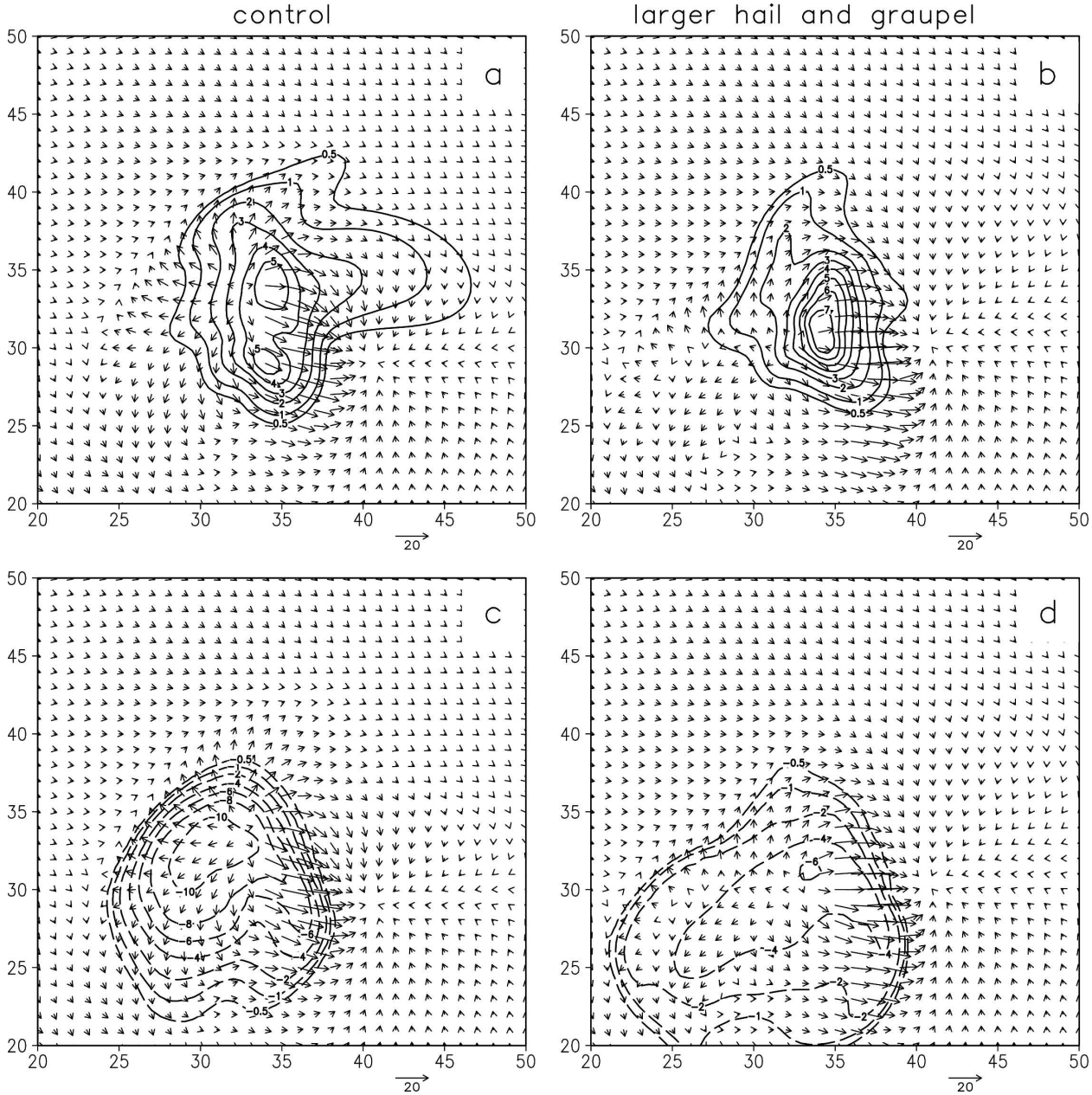

FIG. 11. Rain + hail mixing ratio with perturbation wind vectors at $z = 127$ m, at 45 min for (a) control and (b) large hail and graupel; perturbation equivalent potential temperature with perturbation wind vectors at $z = 127$ m, at 45 min for (c) control and (d) large hail and graupel; perturbation potential temperature with perturbation wind vectors at $z = 127$ m, at 45 min for (e) control and (f) large hail and graupel; upward velocity at $z = 3500$ m (thick) and downward velocity at 525 m (thin) with perturbation wind vectors at $z = 127$ m, at 75 min for (g) control and (h) large hail and graupel. Axes are labeled in km. Contour intervals in (a) and (b) are 1 g kg^{-1}, with an additional contour at 0.5 g kg^{-1}; in (c) and (d) contours are 2 K with additional contours at -0.5 and -1 K; in (e) and (f) contours are 1 K with an additional contour at -0.5 K; and in (g) and (h) contours are 5 K for thick contours and 2 K with an additional contour at -1 K for thin contours, with zero contours omitted. Wind vectors are shown at every other grid point.

ment of peak freezing in the presence of strong upward velocities. In their simulations, however, the updrafts were neither deep enough nor strong enough to carry the smaller hydrometeors to the upper troposphere to form a cirrus anvil. Simulations of stronger and deeper convection by Khain and Pokrovsky (2004) showed a monotonic decrease in the accumulated rain amount with an increase in cloud condensation nuclei (CCN) concentration, consistent with our results. However, outcomes can vary as a result of the interactions be-

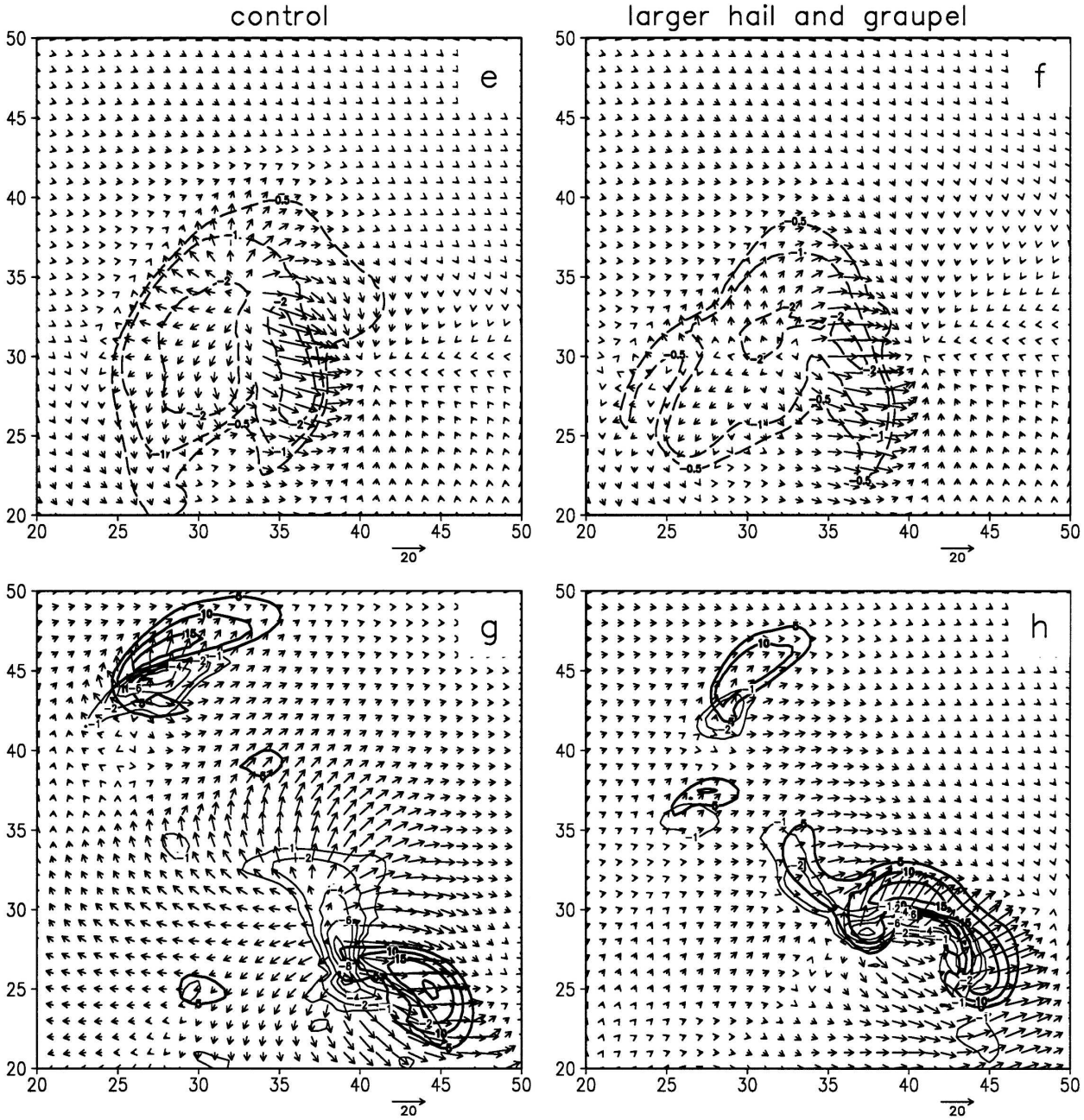

FIG. 11. (*Continued*)

tween the dynamics and microphysics (Khain et al. 2005).

Using a model that is very different from the one used here, Ziegler (1988) found that increasing ν_c had little effect and explained this by saying that the rate of collection of cloud water is primarily dependent on the mean droplet size and very weakly dependent on the relative number of large cloud droplets. This raises the question of whether, in the present simulations, increasing ν_c had any direct effect on the collection rate, or if the smaller collection rate was a consequence of the decreased precipitation resulting from the smaller rate of autoconversion. We therefore repeated the simulations with $\nu_c = 5$ but used $\nu_c = 1$ only for computing the autoconversion rate. The results (not shown) were again substantially different from the control run, with much less collection of cloud water and much more autoconversion, the latter presumably because of the

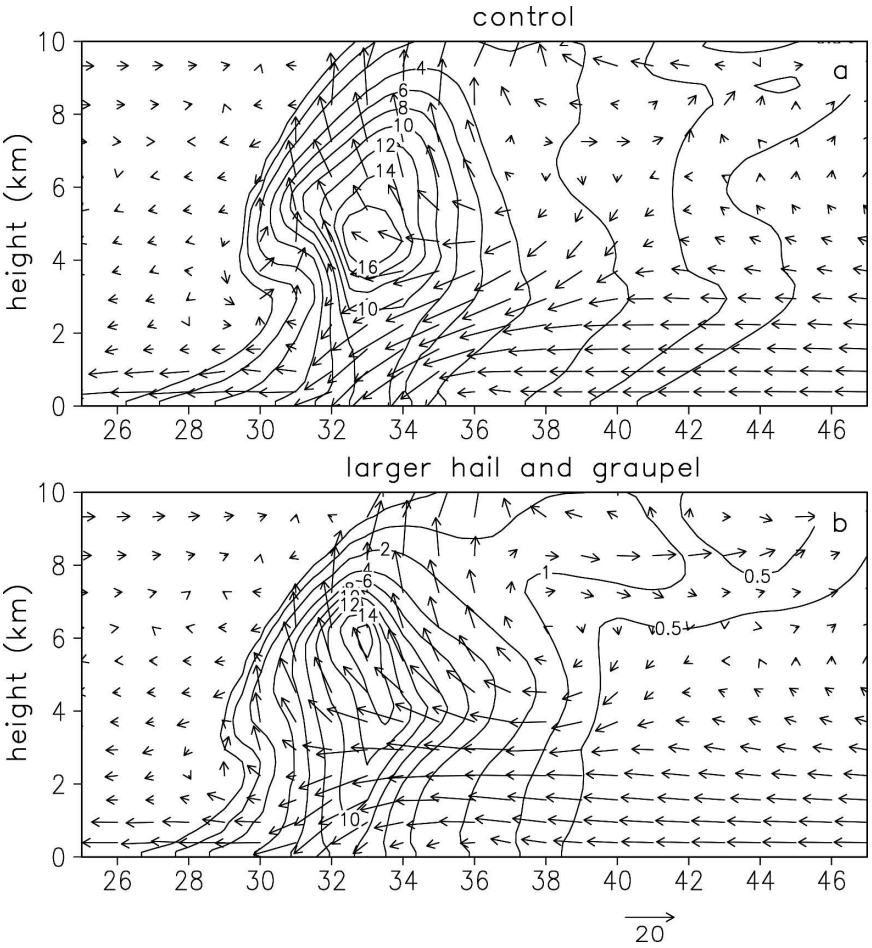

FIG. 12. East–west cross sections of rain + hail + graupel mixing ratio with wind vectors, at 45 min for (a) warm sounding control and (b) warm sounding with large hail and graupel. The contour interval is 2 g kg^{-1}, with additional contours at 0.5 and 1 g kg^{-1}. Axes are labeled in km. Wind vectors are shown at every other horizontal grid point. For each simulation, cross sections are at the latitude with the largest amount of precipitation.

larger availability of cloud water that was not collected. This indicates that increasing ν_c did independently result in significant decreases in the rates of both autoconversion and collection of cloud water. Without making a detailed examination of Ziegler's (1985, 1988) model, we can conclude further that results of some sensitivity tests can be highly dependent on model formulation.

Unlike the results of McCaul et al. (2005), which showed the clouds with warmer soundings to be more variable and therefore perhaps less predictable, the microphysics sensitivity tests show the clouds in colder environments to be more sensitive to changes in N_{tc} or ν_c. With the warmer sounding, which has about twice the precipitable water, more rain is available to collect cloud water, and it exists over a deeper layer. At around 4 km, where the rain is beginning to freeze in the colder cloud (Fig. 14), the rate of collection of cloud water by rain (Fig. 15) is at or is still approaching its maximum in the warmer clouds. More collection produces a positive feedback, as more rain is available to collect cloud water. As explained in McCaul et al. (2005), rain collects more cloud water than does the same mixing ratio of hail, so this positive feedback is more effective in the warmer cloud. Collection of cloud water by rain is delayed with the larger N_{tc} or ν_c for both soundings, but the greater depth warmer than 0°C provides more time for collection to increase in a parcel rising in the warmer clouds.

Therefore, when the rate of collection of cloud water by rain decreases because of the larger N_{tc} or ν_c, there is a smaller fractional decrease in the vertically integrated collection by rain in the warmer cloud. Despite this, the additional amount of cloud water that is still

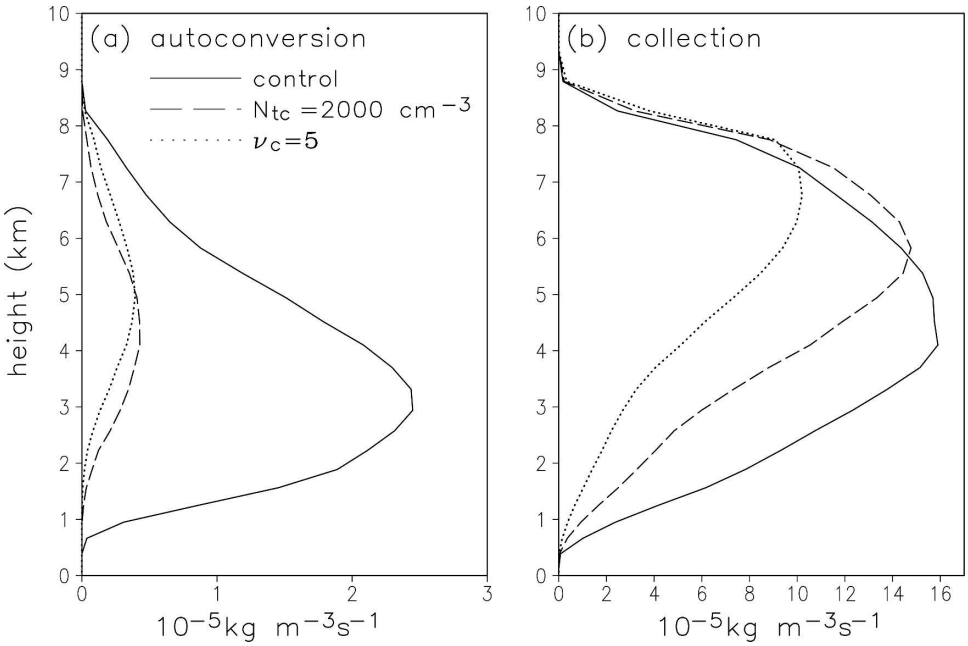

FIG. 13. (a) Autoconversion and (b) collection of cloud water for the control simulation (solid) and for the experiments with N_{tc} = 2000 cm^{-3} (dashed) and ν_c = 5 (dotted), horizontally averaged over the whole domain for the second hour, for the simulations with the cold sounding.

available to be collected is greater when the precipitable water is larger. Comparing the two simulations (Fig. 14) shows that in the warmer cloud the increases in N_{tc} or ν_c result in a smaller decrease in the sum of the heating from freezing of rain and riming of cloud water at around −10°C. The smaller decrease in the growth of hail at that temperature leads to more riming with the larger N_{tc} or ν_c. With the cold sounding, in contrast, the

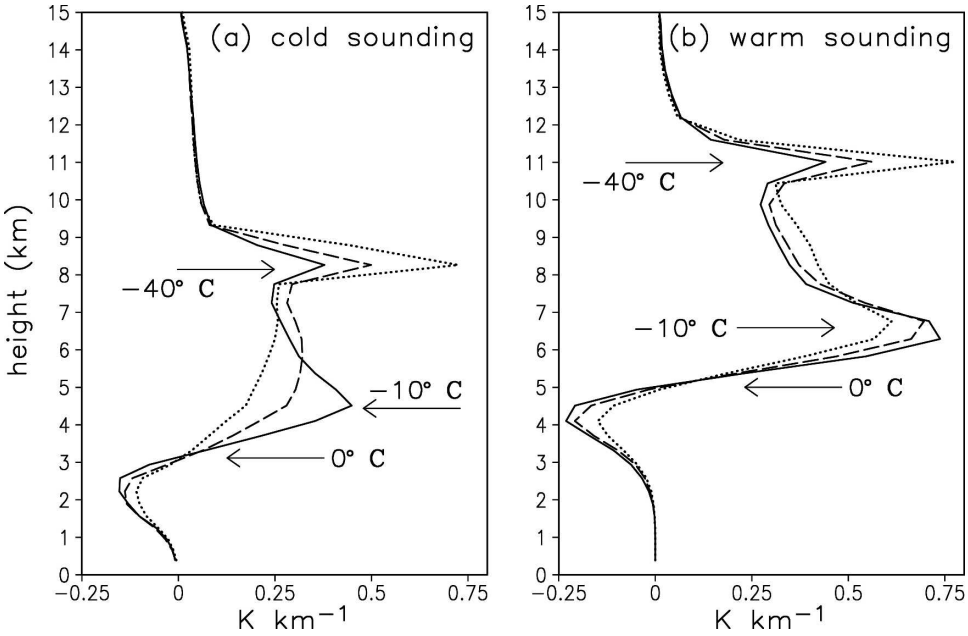

FIG. 14. Release of latent heat of fusion (K km^{-1}) in updrafts for the control simulation (solid) and for the experiments with N_{tc} = 2000 cm^{-3} (dashed) and ν_c = 5 (dotted), horizontally averaged over the whole domain for the second hour, for the simulations with the (a) cold and (b) warm sounding.

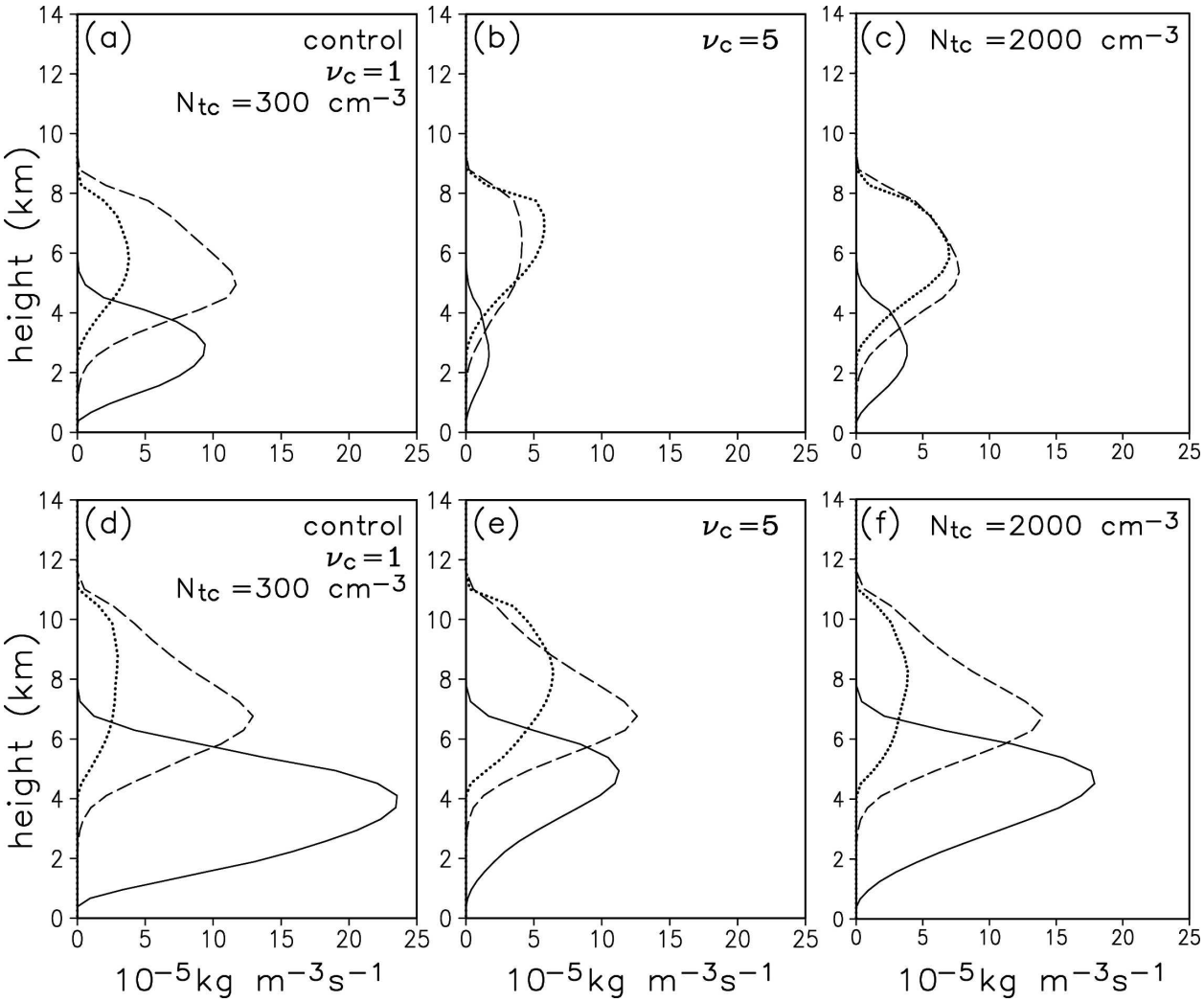

FIG. 15. Collection of cloud water by rain (solid), by hail (dashed), and by graupel (dotted), horizontally averaged over the whole domain for the second hour, for the (a) control simulation, (b) $\nu_c = 5$, (c) $N_{tc} = 2000$ cm^{-3}, for the simulations with the cold sounding, and for the (d) control simulation, (e) $\nu_c = 5$, (f) $N_{tc} = 2000$ cm^{-3}, for the simulations with the warm sounding.

increases in N_{tc} or ν_c result in a significant decrease in the rate of freezing of rain and of riming (evident in the latent heating between $-10°$ and $-40°$C).

Thus, we see that when N_{tc} or ν_c are increased with the warm sounding, the decrease in the rate of hail formation by freezing of rain is less than with the cold sounding, and the additional amount of cloud water that was not collected by rain is larger. Therefore, while the larger N_{tc} or ν_c results in a substantial decrease in the growth of hail by riming with the cold sounding (Fig. 15), this decrease is much less with the warm sounding. Although a much larger rate of growth of graupel by riming compensates for the decrease of riming by hail in the experiments with the cold sounding, graupel does not produce as large a rate of precipitation as does an equal amount of hail. Changing N_{tc} or ν_c has a much smaller effect on the precipitation rate with the warm sounding (Fig. 6).

4. Discussion and conclusions

Results of numerical simulations are most useful when they are determined more by the basic physics than by the parameters that need to be specified despite the lack of adequate data to do so. It is therefore reassuring that in some ways the model results are not very sensitive to changes in the value of ν for precipitating hydrometeors, because of counteracting effects. For example, with a larger value of ν, there is a larger rate of collection of cloud water by precipitation, but also an increased rate of evaporation. With a larger size for hail and graupel, the collection rate decreases, but the

smaller total surface area results in slower melting and less evaporation at low levels. In both situations, there is only a small change in the rate of precipitation at the ground.

However, with a larger value of ν, the greater production of precipitation by collection and the increased evaporation result in more low-level cooling by the downdraft. Specifying larger hail and graupel results in less low-level cooling by the downdraft. The selection of these microphysical parameters must, therefore, be carefully made.

Although the simulation with the cold initial sounding showed a potentially significant change in the speed of storm propagation when $D_{\overline{m}}$ was increased for hail and graupel, this did not occur when the warm initial sounding was used. Based on these few cases, the change in propagation speed should not be considered a general result, but only an example of what is possible.

From (2) and (3), we can see that when N_0 is specified as a constant in an exponential distribution, as in Gilmore et al. (2004a), the values of $D_{\overline{m}}$ and N_t both increase with the mixing ratio of the hydrometeor. Federer and Waldvogel (1975) computed the time variation of N_0 and $\Lambda(=D_n^{-1})$ within an observed storm and found that neither was constant. They concluded, as did Cheng et al. (1985), that there is an inverse relationship between the number and size of hailstones. This inverse relationship cannot be produced in our model because $D_{\overline{m}}$ is held constant, and it cannot occur with a constant N_0, demonstrating a limitation of single-moment schemes.

Gilmore et al. (2004a) rejected the idea of using ensembles of forecasts with different values of microphysics parameters, because of the excessively large range of possible outcomes. This conclusion may be affected by their selection of a very wide range of observed values of N_0 and particle density for both hail and graupel in a single category. Independent of this, another problem with varying microphysical parameters in ensemble forecasts is that we would need to decide which parameters to vary. Although changing N_0 is conceptually different from changing $D_{\overline{m}}$, the outcome may be the same (Gilmore et al. 2004b). Other parameters could be varied, such as particle density, ν, N_t, D_n, the particle habit for pristine crystals, and, as discussed below, CCN.

Figure 9 lends some support to the speculation of Gilmore et al. (2004a) that single-moment schemes with more ice species have less inherent uncertainty. Because larger hail collects less cloud water than an equal mixing ratio of smaller hail, there is more cloud water available to be collected by graupel. This limits our model's overall sensitivity to the specified $D_{\overline{m}}$. In addition, including both hail and graupel as prognostic variables limits the available options for selecting parameters that determine the mean particle size.

Neither N_0 nor $D_{\overline{m}}$ would need to be specified if number concentration were forecast, but it would still be necessary to select the shape of the distribution for each hydrometeor category. As shown here, the results are sensitive to the value of ν for a gamma distribution of hydrometeor diameters, but much more so for cloud water droplets than for precipitating hydrometeors. With a larger ν_c, there is less autoconversion and less collection of cloud water, and consequently much less precipitation at the ground and denser cirrus anvils. To use a cloud-resolving model with a microphysics parameterization for operational forecasting, some decision needs to be made regarding the shapes of the hydrometeor size distributions. Milbrandt and Yau (2005a,b) show the importance of forecasting the shape parameter of a gamma distribution in a three-moment scheme and present a method of forecasting it, but only for sedimenting hydrometeors, not for cloud water.

The model results also show a significant sensitivity to N_{tc}, with differences that are qualitatively the same as with changes to ν_c. Although methods are available to forecast N_{tc} (Saleeby and Cotton 2004; Roelofs and Jongen 2004; Khain et al. 2005), doing so in an operational model would require that models be initialized with 3D fields of CCN, and that sources and sinks of CCN be accounted for. An alternative would be to use CCN as an additional variable in ensemble simulations, when this is expected to change rapidly over space or time. The value of ν_c could also be varied in ensemble simulations.

As discussed in section 2a, modelers need additional data on collection efficiencies for accretion of cloud water. In the future, the collection efficiency could be formulated as a function of the diameters of the collector and collected species, and included within the double integral that is used to compute the lookup tables.

We have shown that the results of simulations using a two-moment microphysics parameterization can show significant sensitivities to quantities that need to be specified but cannot easily be derived from observations. This should motivate researchers to develop more complex microphysics parameterizations that do not have such sensitivities and should provide some guidance to users of models with two-moment schemes.

Acknowledgments. This research is a part of the Convection Morphology Parameter Space Study (COMPASS), which is supported by Grant ATM-

0126408 from the National Science Foundation, under the supervision of Dr. Stephan Nelson. For additional information on the COMPASS study, see our Web site (http://space.hsv.usra.edu/COMPASS). The COMPASS numerical simulations were conducted on the Matrix linux cluster at the University of Alabama in Huntsville (UAH). We also acknowledge programming support from Jayanthi Srikishen of USRA Huntsville, and computer system support from Scott Podgorny, UAH, throughout this project. Matthew Gilmore and Morris Weisman provided helpful reviews of the manuscript.

REFERENCES

Andreae, M. O., D. Rosenfeld, P. Artaxo, A. A. Costa, G. P. Frank, K. M. Longo, and M. A. F. Silva-Dias, 2004: Smoking rain clouds over the Amazon. *Science,* **303,** 1337–1345.

Beard, K. V., and H. T. Ochs, 1984: Collection and coalescence efficiencies for accretion. *J. Geophys. Res.,* **89,** 7165–7169.

——, R. I. Durkee, and H. T. Ochs III, 2002: Coalescence efficiency measurements for minimally charged cloud drops. *J. Atmos. Sci.,* **59,** 233–243.

Brandes, E. A., G. Zhang, and J. Vivekanandan, 2003: An evaluation of a drop distribution–based polarimetric radar rainfall estimator. *J. Appl. Meteor.,* **42,** 652–660.

——, ——, and ——, 2004a: Drop size distribution retrieval with polarimetric radar: Model and application. *J. Appl. Meteor.,* **43,** 461–475.

——, ——, and ——, 2004b: Comparison of polarimetric radar drop size distribution retrieval algorithms. *J. Atmos. Oceanic Technol.,* **21,** 584–598.

Bringi, V. N., G.-J. Huang, V. Chandrasekar, and E. Gorgucci, 2002: A methodology for estimating the parameters of a gamma raindrop size distribution model from polarimetric radar data: Application to a squall-line event from the TRMM/Brazil campaign. *J. Atmos. Oceanic Technol.,* **19,** 633–645.

——, V. Chandrasekar, J. Hubbert, E. Gorgucci, W. L. Randeu, and M. Schoenhuber, 2003: Raindrop size distribution in different climatic regimes from disdrometer and dual-polarized radar analysis. *J. Atmos. Sci.,* **60,** 354–365.

Brooks, H. E., C. A. Doswell III, and R. A. Maddox, 1992: On the use of mesoscale and cloud-scale models in operational forecasting. *Wea. Forecasting,* **7,** 120–132.

Bunkers, M. J., B. A. Klimowski, J. W. Zeitler, R. L. Thompson, and M. L. Weisman, 2000: Predicting supercell motion using a new hodograph technique. *Wea. Forecasting,* **15,** 61–79.

Cheng, L., M. English, and R. Wong, 1985: Hailstone size distributions and their relationship to storm thermodynamics. *J. Climate Appl. Meteor.,* **24,** 1059–1067.

Costa, A. A., C. J. de Oliveira, J. C. P. de Oliveira, and A. J. da Costa Sampaio, 2000: Microphysical observations of warm cumulus clouds in Ceara, Brazil. *Atmos. Res.,* **54,** 167–199.

Crutzen, P. J., 2004: New directions: The growing urban heat and pollution "island" effect—Impact on chemistry and climate. *Atmos. Environ.,* **38,** 3539–3540.

Curic, M., and J. Janc, 1997: On the sensitivity of hail accretion rates in numerical modeling. *Tellus,* **49A,** 100–107.

Eagan, R. C., P. V. Hobbs, and L. F. Radke, 1974a: Particle emissions from a large Kraft paper mill and their effects on the microstructure of warm clouds. *J. Appl. Meteor.,* **13,** 535–552.

——, ——, and ——, 1974b: Measurements of cloud condensation nuclei and cloud droplet size distributions in the vicinity of forest fires. *J. Appl. Meteor.,* **13,** 553–557.

Elmore, K. L., D. J. Stensrud, and K. C. Crawford, 2002a: Ensemble cloud model applications to forecasting thunderstorms. *J. Appl. Meteor.,* **41,** 363–383.

——, ——, and ——, 2002b: Explicit cloud-scale models for operational forecasts: A note of caution. *Wea. Forecasting,* **17,** 873–884.

——, S. J. Weiss, and P. C. Banacos, 2003: Operational ensemble cloud model forecasts: Some preliminary results. *Wea. Forecasting,* **18,** 953–964.

Federer, B., and A. Waldvogel, 1975: Hail and raindrop size distributions from a Swiss multicell storm. *J. Appl. Meteor.,* **14,** 91–97.

Feingold, G., R. L. Walko, B. Stevens, and W. R. Cotton, 1998: Simulations of marine stratocumulus using a new microphysical parameterization scheme. *Atmos. Res.,* **47–48,** 505–528.

Fraile, R., A. Castro, L. Lopez, J. L. Sanchez, and C. Palencia, 2003: The influence of melting on hailstone size distribution. *Atmos. Res.,* **67–68,** 203–213.

Frank, W. M., and C. Cohen, 1985: Properties of tropical cloud ensembles estimated using a cloud model and an observed updraft population. *J. Atmos. Sci.,* **42,** 1911–1928.

Gerber, H., 1996: Microphysics of marine stratocumulus clouds with two drizzle modes. *J. Atmos. Sci.,* **53,** 1649–1662.

Giaiotti, D., E. Gianesini, and F. Stel, 2001: Heuristic considerations pertaining to hailstone size distributions in the plain of Friuli-Venezia Giulia. *Atmos. Res.,* **57,** 269–288.

Gilmore, M. S., J. M. Straka, and E. N. Rasmussen, 2004a: Precipitation uncertainty due to variations in precipitation particle parameters within a simple microphysics scheme. *Mon. Wea. Rev.,* **132,** 2610–2627.

——, S. C. van den Heever, J. M. Straka, R. Wilhelmson, W. R. Cotton, and E. N. Rasmussen, 2004b: Constant slope or constant intercept? The impact on precipitation using single-moment microphysics. *14th Int. Conf. on Clouds and Precipitation*, Bologna, Italy, International Commission on Clouds and Precipitation, 1500–1503. [Available online at http://www.atmos.uiuc.edu/~gilmore1/14ICCP/GVSWCR.pdf.]

Glickman, T. S., Ed., 2000: *Glossary of Meteorology.* 2d ed. Amer. Meteor. Soc., 855 pp.

Khain, A., and A. Pokrovsky, 2004: Simulation of effects of atmospheric aerosols on deep turbulent convective clouds using a spectral microphysics mixed-phase cumulus cloud model. Part II: Sensitivity study. *J. Atmos. Sci.,* **61,** 2983–3001.

——, ——, and I. Sednev, 1999: Some effects of cloud–aerosol interaction on cloud microphysics structure and precipitation formation: Numerical experiments with a spectral microphysics cloud ensemble model. *Atmos. Res.,* **52,** 195–220.

——, M. Ovtchinnikov, M. Pinsky, A. Pokrovsky, and H. Krugliak, 2000: Notes on the state-of-the-art numerical modeling of cloud microphysics. *Atmos. Res.,* **55,** 159–224.

——, D. Rosenfeld, and A. Pokrovsky, 2005: Aerosol impact on the dynamics and microphysics of deep convective clouds. *Quart. J. Roy. Meteor. Soc.,* **131,** 2639–2663.

Kirkpatrick, C., and E. W. McCaul Jr., 2004: The motion of simulated convective storms as a function of basic environmental parameters. Preprints, *22d Conf. on Severe Local Storms,* Hyannis, MA, Amer. Meteor. Soc., CD-ROM, 8A.7.

Lang, S., W.-K. Tao, J. Simpson, and B. Ferrier, 2004: Reply. *J. Appl. Meteor.,* **43,** 962–965.

Liu, Y., and P. H. Daum, 2004: Parameterization of the autoconversion process. Part I: Analytical formulation of the Kessler-type parameterizations. *J. Atmos. Sci.,* **61,** 1539–1548.

Lynn, B. H., A. P. Khain, J. Dudhia, D. Rosenfeld, A. Pokrovsky, and A. Seifert, 2005a: Spectral (bin) microphysics coupled with a mesoscale model (MM5). Part I: Model description and first results. *Mon. Wea. Rev.,* **133,** 44–58.

——, ——, ——, ——, ——, and ——, 2005b: Spectral (bin) microphysics coupled with a mesoscale model (MM5). Part II: Simulation of a CaPE rain event with a squall line. *Mon. Wea. Rev.,* **133,** 59–71.

Martinez, D., and E. G. Gori, 1999: Raindrop size distributions in convective clouds over Cuba. *Atmos. Res.,* **52,** 221–239.

McCaul, E. W., Jr., and C. Cohen, 2002: The impact on simulated storm structure and intensity of variations in the mixed layer and moist layer depths. *Mon. Wea. Rev.,* **130,** 1722–1748.

——, ——, and C. Kirkpatrick, 2005: The sensitivity of simulated storm structure, intensity, and precipitation efficiency to the temperature at the lifted condensation level. *Mon. Wea. Rev.,* **133,** 3015–3037.

McCumber, M., W.-K. Tao, J. Simpson, R. Penc, and S.-T. Soong, 1991: Comparison of ice-phase microphysical parameterization schemes using numerical simulations of tropical convection. *J. Appl. Meteor.,* **30,** 985–1004.

Meyers, M. P., R. L. Walko, J. Y. Harrington, and W. R. Cotton, 1997: New RAMS cloud microphysics parameterization. Part II: The two-moment scheme. *Atmos. Res.,* **45,** 3–39.

Milbrandt, J. A., and M. K. Yau, 2005a: A multimoment bulk microphysics parameterization. Part I: Analysis of the role of the spectral shape parameter. *J. Atmos. Sci.,* **62,** 3051–3064.

——, and ——, 2005b: A multimoment bulk microphysics parameterization. Part II: A proposed three-moment closure and scheme description. *J. Atmos. Sci.,* **62,** 3065–3081.

Miles, N. L., J. Verlinde, and E. E. Clothiaux, 2000: Cloud droplet size distributions in low-level stratiform clouds. *J. Atmos. Sci.,* **57,** 295–311.

Mitchell, D. L., S. K. Chai, Y. Liu, A. J. Heymsfield, and Y. Dong, 1996: Modeling cirrus clouds. Part I: Treatment of bimodal size spectra and case study analysis. *J. Atmos. Sci.,* **53,** 2952–2966.

Nzeukou, A., H. Sauvageot, A. D. Ochou, C. Mouhamed, and F. Kebe, 2004: Raindrop size distribution and radar parameters at Cape Verde. *J. Appl. Meteor.,* **43,** 90–105.

Pielke, R. A., and Coauthors, 1992: A comprehensive meteorological modeling system—RAMS. *Meteor. Atmos. Phys.,* **49,** 69–91.

Roelofs, G.-J., and S. Jongen, 2004: A model study of the influence of aerosol size and chemical properties on precipitation formation in warm clouds. *J. Geophys. Res.,* **109,** D22201, doi:10.1029/2004JD004779.

Rosenfeld, D., 1999: TRMM observed first direct evidence of smoke from forest fires inhibiting rainfall. *Geophys. Res. Lett.,* **26,** 3105–3108.

——, 2000: Suppression of rain and snow by urban and industrial air pollution. *Science,* **287,** 1793–1796.

Saleeby, S. M., and W. R. Cotton, 2004: A large-droplet mode and prognostic number concentration of cloud droplets in the Colorado State University Regional Atmospheric Modeling System (RAMS). Part I: Module descriptions and supercell test simulations. *J. Appl. Meteor.,* **43,** 182–195.

Straka, J. M., and E. R. Mansell, 2005: A bulk microphysics parameterization with multiple ice precipitation categories. *J. Appl. Meteor.,* **44,** 445–466.

Tao, W.-K., and Coauthors, 2003: Microphysics, radiation and surface processes in the Goddard Cumulus Ensemble (GCE) model. *Meteor. Atmos. Phys.,* **82,** 97–137.

Tokay, A., and D. A. Short, 1996: Evidence from tropical raindrop spectra of the origin of rain from stratiform versus convective clouds. *J. Appl. Meteor.,* **35,** 355–371.

Tripoli, G. J., and W. R. Cotton, 1981: The use of ice-liquid water potential temperature as a thermodynamic variable in deep atmospheric models. *Mon. Wea. Rev.,* **109,** 1094–1102.

Uijlenhoet, R., M. Steiner, and J. A. Smith, 2003: Variability of raindrop size distributions in a squall line and implications for radar rainfall estimation. *J. Hydrometeor.,* **4,** 43–61.

Ulbrich, C. W., 1983: Natural variations in the analytical form of the raindrop size distribution. *J. Climate Appl. Meteor.,* **22,** 1764–1775.

van den Heever, S. C., and W. R. Cotton, 2004: The impact of hail size on simulated supercell storms. *J. Atmos. Sci.,* **61,** 1596–1609.

Walko, R. L., W. R. Cotton, M. P. Meyers, and J. Y. Harrington, 1995: New RAMS cloud microphysics parameterization. Part I: The single-moment scheme. *Atmos. Res.,* **38,** 29–62.

Zhang, G., J. Vivekanandan, E. A. Brandes, R. Meneghini, and T. Kozu, 2003: The shape–slope relation in observed gamma raindrop size distributions: Statistical error or useful information? *J. Atmos. Oceanic Technol.,* **20,** 1106–1119.

Ziegler, C. L., 1985: Retrieval of thermal and microphysical variables in observed convective storms. Part I: Model development and preliminary testing. *J. Atmos. Sci.,* **42,** 1487–1509.

——, 1988: Retrieval of thermal and microphysical variables in observed convective storms. Part II: Sensitivity of cloud processes to variation of the microphysical parameterization. *J. Atmos. Sci.,* **45,** 1072–1090.